

# Comparison of GA and DDE for optimizing coverage in indoor environment

Shu-Han Liao, Chien-Ching Chiu<sup>\*†</sup> and Min-Hui Ho

*Department of Electrical Engineering, Tamkang University, Tamsui, Taiwan*

## SUMMARY

This paper presents a method for determining the required number and locations of transmitting antennas to optimize wireless propagation coverage in indoor ultra-wideband communication system. In the coverage prediction model, we use the three-dimensional ray-tracing technique associated to a genetic algorithm and a dynamic differential evolution for optimizing the transmitting antennas location in an indoor environment. The ray-tracing method is employed to calculate the field strength from one or more transmitting antennas, and the optimization algorithm is used to determine the required number and locations of these antennas to achieve optimized wireless coverage in the indoor environment. The combined three-dimensional ray-tracing and optimization algorithm was applied in the indoor environment to find the best location of the transmitting antennas by maximizing the power in the coverage area. The use of deployments to minimize the transmitting antennas and maximize the power in the coverage area was proposed. Obtained simulation results illustrate the feasibility of using the integrated ray-tracing and optimization method to find the optimal transmitter locations in determining the optimized coverage of a wireless network. The dynamic differential evolution has better optimization results compared with the genetic algorithm. The investigated results can help communication engineers improve their planning and design of indoor wireless communication. Copyright © 2013 John Wiley & Sons, Ltd.

Received 25 September 2012 Revised 21 January 2013 Accepted 13 February 2013

KEY WORDS: UWB; genetic algorithm; dynamic differential evolution; power; ray-tracing

## 1. INTRODUCTION

According to the Federal Communication Commission, ultra-wideband (UWB) signal is defined as a signal having fractional bandwidth greater than 20% of the center frequency [1–5]. In the design of indoor wireless communications, the number and locations of transmitting antennas are crucial for obtaining optimal coverage. To this end, a thorough understanding of wireless propagation in indoor communication system of interest is necessary. Because of the often complex indoor propagation environments, intensive measurements are commonly used to collect data and build empirical propagation models that could be used to determine the number and locations of transmitting antennas and establish adequate coverage in regions of interest. In [6], the model proposes a two-dimensional ray-tracing [7–17] prediction technique associated with a real-coded mono-objective genetic algorithm (GA). The GA provides results for antenna position optimization that maximizes the lower field values.

In the paper, the GA and dynamic differential evolution (DDE) optimization methods have been used in the determination of the locations of transmitting antennas and three-dimensional ray-tracing methods used in the design and optimization of the locations of transmitting antennas, none of these methods provided an integrated approach that leads to the determination of an optimized wireless coverage. The three-dimensional ray-tracing model used here is based on image theory

<sup>\*</sup>Correspondence to: Chien-Ching Chiu, Department of Electrical Engineering, Tamkang University, Tamsui, Taiwan.

<sup>†</sup>E-mail: chiu@ee.tku.edu.tw

to precisely consider all the electromagnetic waves paths leaving the transmitting antennas and reaching the receiving antennas. The fields are computed at all receiving antennas, which are uniformly distributed in the indoor environment. Then, it is possible to estimate the power strength received by transmitting antennas at each antenna position of the environment. The GA and DDE techniques are developed to optimize transmitter positions in an indoor environment, taking into account the coverage and number of transmitting antenna. The GA and DDE algorithms are coupled with three-dimensional ray-tracing propagation that provides accurate field predictions to address the wireless coverage optimization issue. The ray-tracing combined optimization algorithm was used to determine the required number and locations of transmitting antennas to ensure effective wireless coverage in a given propagation environment. The cost function of the algorithm is a set of electric field values computed over the region of interest for a certain antenna location. The goal is to find the optimal antenna position that maximizes the received power in the coverage area, resulting in more than the total received fields. The paper focuses on random deployments of transmitting antennas in the indoor environment. For the purpose of the investigation, an evolutionary optimization algorithm is developed to focus on minimizing the transmitting antennas and maximizing the power in the coverage area.

The remaining sections of this paper are organized as follows: Section 2 presents a brief overview of the system description. Sections 3 and 4 describe the GA and DDE, respectively. The numerical results are then presented in Section 5. The simulation environment and the comparison of the algorithm are also described. The conclusion is made in Section 6.

## 2. SYSTEM DESCRIPTION

The shooting and bouncing ray/image (SBR/Image) method can deal with high-frequency radio wave propagation in the complex indoor environments [18, 19]. Using ray-tracing techniques to predict channel characteristic is effective and fast [18–20]. Thus, a ray-tracing channel model is developed to calculate the channel matrix of UWB system.

By using these images and received fields, we can obtain the channel frequency response as follows:

$$H(f) = \sum_{i=1}^{M_T} a_i(f) e^{j\theta_i(f)} \quad (1)$$

where  $f$  is the frequency of the sinusoidal wave,  $i$  is the path index,  $M_T$  is the total number of paths,  $\theta_i$  is the  $i$ th phase shift, and  $a_i$  is the  $i$ th receiving magnitude. Note that the receiving antenna in our simulation is an omnidirectional UWB dipole antenna. On the other hand, the transmitter is the UWB antenna that has been described in the previous section. The channel frequency response of UWB can be calculated from ((1)) in the frequency range of UWB.

The frequency response is transformed to the time domain by using the inverse fast Fourier transform with the Hermitian signal processing [21]. Therefore, the time-domain impulse response of the equivalent baseband can be written as follows:

$$h_b(t) = \sum_{m=1}^{M_T} \alpha_m \delta(t - \tau_m) \quad (2)$$

where  $m$  is the path index and  $M_T$  is the total number of paths.  $\alpha_m$  and  $\tau_m$  are the channel gain and time delay for the  $m$ th path, respectively.

The ray-tracing method implemented in these simulations has been shown accurate and computationally efficient in the calculation of coverage and other communications parameters. These features have been used in the calculation of the optimized coverage simulations presented in this paper.

## 3. GENETIC ALGORITHM

The GA is the global numerical optimization methods based on genetic recombination and evaluation in nature [22, 23]. They use the iterative optimization procedures, which start with a

randomly selected population of potential solutions. Then, they gradually evolve toward a better solution through the application of the genetic operators. GA typically operates on a discretized and coded representation of the parameters rather than on the parameters themselves. These representations are often considered to be ‘chromosomes’, whereas the individual element, which constitutes chromosomes, is the ‘gene’. Simple but often very effective chromosome representations for optimization problem involving several continuous parameters can be obtained through the juxtaposition of discretized binary representations of the individual parameter.

We regulate the transmitter antenna location of the indoor environment to maximize the received power. The GA starts with a population containing a total of  $G_p$  candidates (i.e.,  $G_p$  is the population size). Each candidate is described by a chromosome. Then, the initial population can simply be created by taking  $G_p$  random chromosomes. GA iteratively generates a new population, which is derived from the previous population through the application of the reproduction, crossover, and mutation operators.

The GA is used to maximize the following cost function:

$$\text{cost function} = \frac{1}{\text{Average Received Power}} \quad (3)$$

where cost function is the inverse of the average received power for UWB system. Through repeated applications of reproduction, crossover, and mutation operators, the initial population is transformed into a new population in an iterative manner. New populations will contain increasingly better chromosomes and will eventually converge to an optimal population that consists of the optimal chromosomes.

As for the GA calculations, each chromosome is assigned information of the position of transmitter as the optimization variables. A binary GA is applied, and a population of 30 chromosomes is used at each generation. For each generated chromosome, the GA reruns the three-dimensional ray-tracing program to calculate the received power at every receiver point from the given location of transmitter as provided by the chromosome. The cost function (criterion for measuring the effectiveness of the obtained optimized GA solution) is chosen as the number of the receiver points where the received power from any transmitter is less than  $-40$  dB. These receiver points are called bad receiver points, and the areas associated with them are called bad receiving-signal area in this paper. Therefore, GA chooses the optimized positions of a given number of transmitters to minimize bad receiving-signal points.

In our simulation, when the cost function is smaller than the threshold value or GA does not find a better individual within 300 successive generations, the GA will be terminated, and a solution is then obtained.

#### 4. DYNAMIC DIFFERENTIAL EVOLUTION

The standard DE algorithm, belonging to the family of evolutionary algorithms, was first proposed by Storn and Price [24]. DE uses genetic operators, referred to as mutation, crossover, and selection. The role of the genetic operators is to ensure that there is sufficient pressure to obtain even better solutions from good ones (exploitation) and to cover sufficiently the solution space to maximize the probability of discovering the global optimum (exploration). DDE algorithm is similar with DE. DDE algorithm starts with an initial population of potential solutions that is composed of a permittivity distribution. Each individual in DDE algorithm is a  $D$ -dimensional vector consisting of  $D$  optimization parameters. DDE algorithm goes through six procedures as follows:

- (1) Initialize a starting population: Individuals in DDE algorithm represent a set of  $D$ -dimensional vectors in the parameter space for the problem,  $\{x_i: i = 1, 2, \dots, N_p\}$ , where  $D$  is the number of parameters to be optimized and  $N_p$  is the population size.
- (2) Evaluate the population using the cost function: After initialization, DDE algorithm evaluates the cost function ((3)) for each individual in the population.

- (3) Perform mutation operation to generate trial vectors: The mutation operation of DDE algorithm is performed by arithmetical combination of individual. For each parameter vector  $X_i^g$  of the parent generation, a trial vector  $X_i^{g+1}$  is generated according to following equation:

$$\begin{aligned} (X_j^{g+1})_i &= (X_j^g)_i + \chi \cdot [(X_{\text{best}}^g)_i - (X_j^g)_i] + \zeta \cdot [(X_m^g)_i - (X_n^g)_i] \\ m, n &\in [0, N_p - 1], m \neq n \end{aligned} \quad (4)$$

where  $\chi$  and  $\zeta$  are the scaling factors associated with the vector differences  $(X_{\text{best}}^g - X_j^g)$  and  $(X_m^g - X_n^g)$ , respectively. The disturbance vector  $X$  due to the mutation mechanism consists of the parameter vector  $X_j^g$ , the best particle  $X_{\text{best}}^g$ , and two randomly selected vectors. As compared with the typical DE [25], the convergence can be accelerated by (4).

- (4) Perform crossover operation with the probability of crossover CR to deliver crossover vectors: The crossover operation in DDE algorithm is performed to increase the diversity of the parameter vectors. This operation is similar to the crossover process in GAs. However, the crossover operation in DDE algorithm only allows to deliver the crossover vector  $u_i$  by mixing the component of the current vector  $x_i^g$  and the trial vector  $x_i^{g+1}$ . It can be expressed as follows:

$$u_i^{g+1}(j) = \begin{cases} x_i^{g+1}(j), & \text{if } \text{Rand}(j) < CR \\ x_i^g(j), & \text{otherwise} \end{cases} \quad (5)$$

where CR is the probability of the crossover,  $CR \in (0,1)$ .  $\text{Rand}(j)$  is the random number generated uniformly between 0 and 1.

- (5) Perform selection operation to produce offspring: Selection operation is conducted by comparing the parent vector  $x_i^g$  with the crossover vectors  $u_i^{g+1}$ . The vector with the smaller cost function value is selected as a member of the next generation. Explicitly, the selection operation for the minimization problem is given by

$$x_i^{g+1} = \begin{cases} u_i^{g+1}, & \text{if } CF(u_i^{g+1}) < CF(x_i^g) \\ x_i^g, & \text{otherwise} \end{cases} \quad (6)$$

The DDE algorithm is carried out in a dynamic way: Each parent individual will be replaced by his offspring immediately if the offspring has a better cost function value than its parent individual does.

- (6) Stop the process and obtain the best individual if the termination criterion is satisfied; otherwise, go to step 2.

The key distinction between a DDE algorithm and a typical DE [24] is on the population updating mechanism. In a typical DE, all the update actions of the population are performed at the end of the generation, of which the implementation is referred as static updating mechanism. Alternatively, the updating mechanism of a DDE algorithm is carried out in a dynamic way: Each parent individual will be replaced by his offspring immediately if the offspring has a better cost function value than its parent individual does. Thus, DDE algorithm can respond to the progress of population status immediately and yield faster convergence speed than the typical DE. On the basis of the convergence property of the DDE algorithm, we are able to reduce the number of cost function evaluations and maximize the received power efficiently.

The three-dimensional SBR/Image method combined DDE algorithm has been presented in this paper. Then, the DDE is used to search the transmitter antenna positions to maximize the received power of the communication system. This technique is used to calculate the UWB channel impulse response for each location of the receiver. On the basis of the channel impulse response, the number of multipath components, the root mean square (RMS) delay spread  $\tau_{\text{RMS}}$ , and the mean excess delay  $\tau_{\text{MED}}$  are computed. The DDE algorithm iteratively

generates a new population with offspring from the previous population through the application of the reproduction by mutation and replacement operators. In our simulation, when the cost function is smaller than the threshold value or the DDE does not find a better individual within 300 successive generations, the DDE will be terminated, and a solution is then obtained.

## 5. NUMERICAL RESULTS

A ray-tracing technique is developed to calculate the channel parameter from 3.1 to 10.6 GHz with frequency interval of 5 MHz. That is, 1501 frequency components are used. Because the dielectric constant and conductivity of the materials changes with frequency, the different values of dielectric constant and conductivity of materials for different frequencies are carefully considered in channel calculation [26–30]. The objective of this paper is to demonstrate the effectiveness of an integrated algorithm and three-dimensional ray tracing in optimizing the wireless coverage in a given propagation environment. Figure 1 is the second floor in Tamkang University, and the floor plan has dimensions of 31.1 (length)  $\times$  39 (width)  $\times$  3 m (height). The building walls are made of concrete block wall with thickness of 0.1 m. The floor plan of the simulated environment is shown in Figure 1. The transmitting antenna is located in the center of the indoor environment at  $\text{TX}_{\text{Center}}$  (19.5, 15.55, and 1.2 m) with the fixed height of 1.2 m. The transmitter is mobile, and the receivers are with uniform interval distribution and a fixed height of 1 m in the whole indoor environment, in which 120 receiving antennas with 3.4-m spacing between adjacent antennas was carried out. The locations of receiving antennas are placed in each laboratory and hallway. At each receiving antenna, the received power is calculated using the ray-tracing method. The transmitting and receiving antennas are UWB antennas.

A three-dimensional SBR/Image technique combined with optimization algorithm has been presented in this paper. The transmitters are searched of the indoor environment and receiving antennas at which the fields are being calculated. This technique is used to calculate the UWB channel impulse response for each location of the receiver. On the basis of the channel impulse response, the number of multipath components, the RMS delay spread  $\tau_{\text{RMS}}$ , and the mean excess delay  $\tau_{\text{MED}}$  are computed.

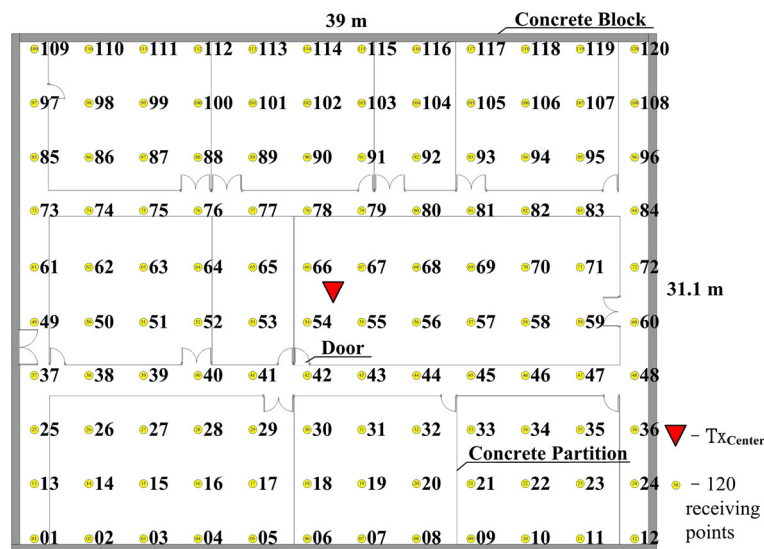


Figure 1. A plan view of the simulated environment.

The cumulative distributions of the RMS delay spread  $\tau_{\text{RMS}}$  is defined as follows [30]:

$$\tau_{\text{RMS}} = \sqrt{\frac{\sum_{n=1}^N \tau_n^2 |a_n|^2}{G} - \left( \frac{\sum_{n=1}^N \tau_n |a_n|^2}{G} \right)^2} \tag{7}$$

where  $G = \sum_{n=1}^N |a_n|^2$  is the total multipath gain.

The mean excess delay,  $\tau_{\text{MED}}$  is defined as [31]:

$$\tau_{\text{MED}} = \frac{\sum_{n=1}^N \tau_n |a_n|^2}{G} \tag{8}$$

By (7) and (8), we can obtain the RMS delay spreads and mean excess delay for those two algorithms.

The specifications of the parameters are set as follows: The operation frequency is 3.1–10.6 GHz. Then, the unknown coefficients are described by a 10-bit string (chromosome). The parameters of the DDE are set as follows: The crossover rate  $\text{CR} = 0.6$ . The scaling factors of  $\chi$  and  $\zeta$  are both 0.8 and the population size  $N_p = 30$ . The parameters of the GA are set as follows: The crossover rate is 0.6, the mutation probability is 0.025, and the population size is 30.

We assume that only one transmitting antenna is available, and the GA and DDE optimization are performed. The position of the transmitter is shown in Figure 2 with only one transmitter. The triangle in Figure 3(a) shows that the transmitting antenna  $\text{TX}_{\text{Center}}$  (19.5, 15.55, and 1.2 m) is located in the center of the indoor environment. In this case, 10 bad receiving-signal points (below  $-40$  dB) occurred including (not highlighted in figure) the receiver points 1, 12, 13, 24, 25, 85, 97, 108, 109, and 120. As shown (circle) in Figure 3(b), the  $\text{TX}_{\text{GA}}$  (21.88, 17.21, and 1.2 m) is

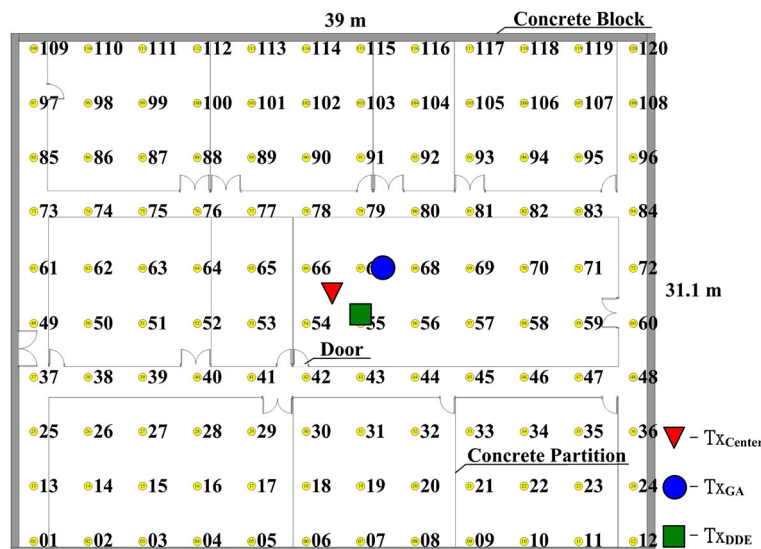


Figure 2. Optimized transmitter position when only one transmitter is used. ( $\blacktriangledown$ ) is the transmitter position  $\text{TX}_{\text{Center}}$  located in the center of the indoor environment, ( $\bullet$ ) is the GA-optimized transmitter position  $\text{TX}_{\text{GA}}$ , and ( $\blacksquare$ ) is the DDE-optimized transmitter position  $\text{TX}_{\text{DDE}}$ .

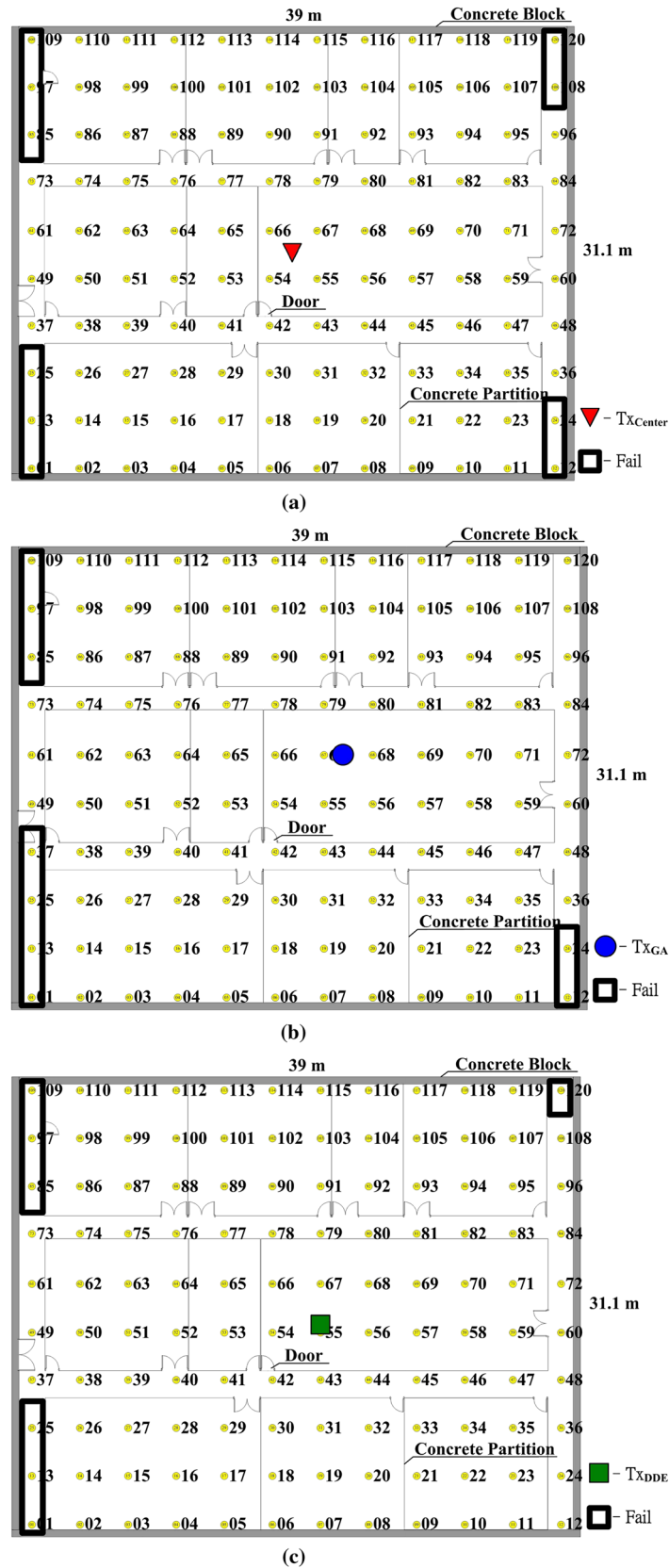


Figure 3. Bad receiving areas (received power below  $-40$  dB) with the use of one transmitter. (a)  $TX_{Center}$ , (b)  $TX_{GA}$ , and (c)  $TX_{DDE}$ .

chosen as the transmitter position by GA. In this case, nine bad receiving-signal points occurred including the receiver points 1, 12, 13, 24, 25, 37, 85, 97, and 109. It is found that the optimized position of the transmitter is located in TX<sub>DDE</sub> (21, 13.9, and 1.2 m) by DDE, as shown by the square in Figure 3(c). The obtained coverage results show that the transmit location causes seven bad receiving-signal points 1, 13, 25, 85, 97, 109, and 120.

We increase the number of transmitters to provide adequate wireless coverage over the entire floor area. The two optimal transmitting antennas are searched in the whole space directly. GA and DDE optimization are performed with two transmitters. The positions of the transmitter are shown in Figure 4 with two transmitters. In the GA optimization, the transmitter points TX<sub>GA</sub> (15.44, 14.77, and 1.2 m) and TX<sub>GA</sub> (20.95, 16.45, and 1.2 m) are chosen as the two transmitter locations as illustrated by the circles, and no bad receiving-signal point exists. In the DDE optimization, the resulting optimized positions TX<sub>DDE</sub> (15.27, 16.2, and 1.2 m) and TX<sub>DDE</sub> (21.08, 13.85, and 1.2 m) are chosen as the two transmitter locations as illustrated by the squares, and no bad receiving-signal point exists. GA and DDE optimization are using two transmitters to help eliminate bad receiving-signal points. These results show that two transmitters are sufficient to provide adequate wireless coverage over the entire floor area when the transmitters are located in the optimized position. Clearly, whereas other combination of the two transmitter positions to cover the entire floor area may be possible, the simulation results show one possible successful solution.

Table 1 shows a summary of the obtained results of the number of bad receiving-signal points for GA and DDE optimization cases as illustrated in Figures 3(a)–(c) and 4. As it may be observed in Table 1, 10 bad receiving-signal points are serious when only one transmitter TX<sub>Center</sub> located in the center of the indoor environment is used. Compared with the number of bad receiving-signal points for GA and DDE algorithm, the DDE has less bad receiving-signal points than the GA.

Table 1 also shows that the number of bad receiving-signal points decreases when using the DDE as the transmitting antenna. The two transmitters used in the simulations have shown that the entire floor area is adequately covered with wireless signals and without any bad receiving-signal point.

To determine the multipath effect, the  $\tau_{RMS}$  and  $\tau_{MED}$  were calculated. Table 2 shows that the RMS delay spread  $\tau_{RMS}$  decreases when using the DDE as the transmitting antenna in the one transmitter and two transmitters. For one transmitter, the  $\tau_{RMS}$  for GA and DDE is 14.1 and 13.94 ns, respectively. It is clear that  $\tau_{RMS}$  for the DDE is the smallest. A summary of these values is given

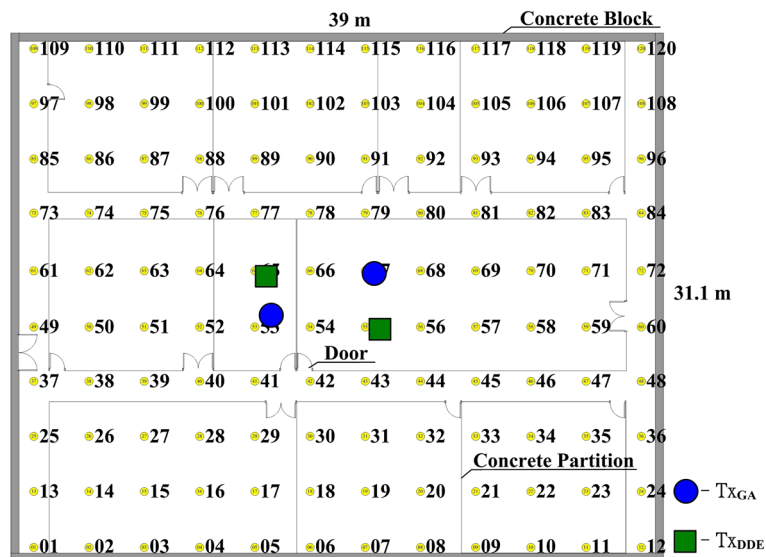


Figure 4. Optimized transmitter positions when two transmitters are used. (●) is the GA-optimized transmitter position TX<sub>GA</sub> and (■) is the DDE-optimized transmitter position TX<sub>DDE</sub>.



Table I. Number of bad receiving-signal points optimized by GA and DDE.

Number of transmitting antenna	Number of bad receiving-signal points		
	$\text{TX}_{\text{Center}}$	$\text{TX}_{\text{GA}}$	$\text{TX}_{\text{DDE}}$
1	10	9	7
2	Nonexistent	0	0

GA, genetic algorithm; DDE, dynamic differential evolution.

Table II. Transmitter channel parameters  $\tau_{\text{MED}}$  and  $\tau_{\text{RMS}}$  of GA and DDE.

Number of transmitting antenna	GA		DDE	
	$\tau_{\text{MED}}$ (ns)	$\tau_{\text{RMS}}$ (ns)	$\tau_{\text{MED}}$ (ns)	$\tau_{\text{RMS}}$ (ns)
1	4.34	14.10	4.15	13.94
2	4.16	13.79	4.04	13.35

MED, mean excess delay; RMS, root mean square; GA, genetic algorithm; DDE, dynamic differential evolution.

in Table 2 for one transmitter and two transmitters, respectively, which clearly shows that the  $\tau_{\text{MED}}$  increase for the GA case.

These simulation examples illustrate features and capabilities of the developed integrated GA and DDE approaches for optimizing wireless coverage in a given propagation area. It should be noted that the algorithm provides global optimization and saves significant computation time compared with, for example, the exhaustive search method.

The average received power versus generations for one transmitter is shown in Figure 5. It is found that the average received power increases quickly by the DDE, and good convergences are achieved within 65 generations. The cost function of DDE is about  $-35.22$  dB in final generation. As a result, the average received power can be increased substantially in indoor UWB communication system.

The average received power versus generations for two transmitters is shown in Figure 6. It is shown that the DDE scheme is able to achieve good convergences within 61 generations. The cost function of DDE is about  $-33.98$  dB in the final generation. The DDE has better optimization results compared with the GA, and numerical results also show that the DDE outperforms the GA in convergence speed.

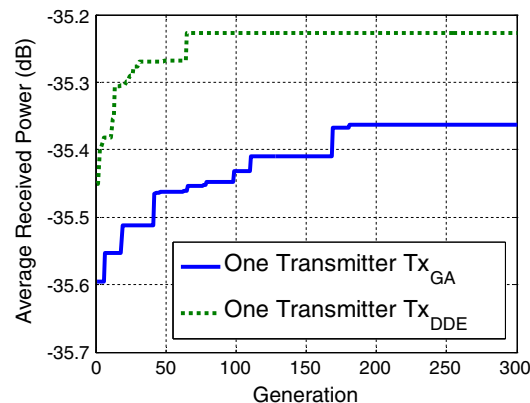


Figure 5. Average received power versus generations by two different algorithms when only one transmitter is used.

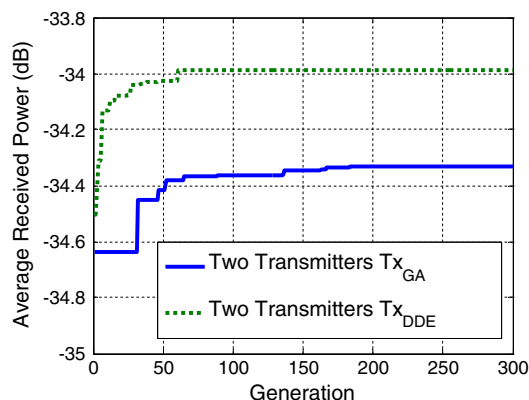


Figure 6. Average received power versus generations by two different algorithms when two transmitters are used.

## 6. CONCLUSIONS

The optimization of coverage of wireless communication networks is studied for an indoor environment. Using the GA and DDE to minimize the transmitting antennas and maximize the power in the coverage area is presented. In this paper, the cost function is defined as the inverse of average received power for UWB system. The GA and DDE minimize the cost function by adjusting the transmitter antenna location. To accurately calculate the wireless coverage, the site-specific ray-tracing method is employed. Channel propagation environments are simulated taking into account for the detailed topology of the propagation site. To obtain optimal coverage for a given number of transmitters, the algorithms GA and DDE were used to determine the best locations of transmitters. As an original contribution, this paper proposes the use of a three-dimensional ray-tracing model for field prediction in indoor wireless systems, associated with GA and DDE for optimizing the transmitter antenna location in this system. It is shown that the combination of the ray-tracing method and the algorithms can lead to optimized coverage even in challenging propagation environments. Numerical results show that the DDE outperforms the GA in convergence speed. As a result, the average received power can be increased substantially in indoor UWB communication system.

## REFERENCES

1. Federal Communications Commission, "Revision of Part 15 of the Commission's Rules Regarding Ultra-Wideband Transmission System, First Report and Order," *FCC, ET Docket*, Feb. 14, 2002; 1–118.
2. Liao SH, Chiu CC, Ho MH, Liu CL. Channel capacity of multiple-input multiple-output ultra wide band systems with single co-channel interference. *International Journal of Communication Systems* Dec 2010; **23**(12): 1600–1612.
3. Lie JP, Ng BP, Meng C See S. Direction finding receiver for UWB impulse radio signal in multipath environment. *International Journal of Communication Systems* Dec 2010; **23**(12):1537–1553.
4. Zhang Z, Lu Z, Chen Q, Yan X, Zheng L-R. Code division multiple access/pulse position modulation ultra-wideband radio frequency identification for Internet of Things: concept and analysis. *International Journal of Communication Systems* Sept 2012; **25**(9):1103–1121.
5. Dariush A-M, Vahid TV. Characterization of indoor time reversal UWB communication systems: spatial, temporal and frequency properties. *International Journal of Communication Systems* Mar 2011; **24**(3):277–294.
6. Grubisic S, Carpes WP, Jr., Bastos JPA. Optimization model for antenna positioning in indoor environments using 2-D ray-tracing technique associated to a real-coded genetic algorithm. *IEEE Transactions Magnetics* 2009; **45**(3):1626–1629.
7. Ho MH, Chiu CC, Liao SH. Optimization of channel capacity for MIMO smart antenna using particle swarm optimizer. *IET Communications* Nov. 2012; **6**(16):2645–2563.
8. Chiu CC, Chen CH, Liao SH, Chen KC. Bit error rate reduction by smart UWB antenna array in indoor wireless communication. *Journal of Applied Science and Engineering* Jun. 2012; **15**(2):139–148.
9. Ho MH, Chiu CC, Liao SH. Bit error rate reduction for circular ultrawideband antenna by dynamic differential evolution. *International Journal of RF and Microwave Computer-Aided Engineering* Mar. 2012; **22**(2):260–271.

10. Chiu CC, Chen CH, Liao SH, Tu TC. Ultra-wideband outdoor communication characteristics with and without traffic. *EURASIP Journal on Wireless Communications and Networking* Mar. 2012; **92**.
11. Liao SH, Ho MH, Chiu CC, Lin CH. Optimal relay antenna location in indoor environment using particle swarm optimizer and genetic algorithm. *Wireless Personal Communications* Feb. 2012; **62**(3):599–615.
12. Chiu CC, Kao YT, Liao SH, Huang YF. UWB communication characteristics for different materials and shapes of the stairs. *Journal of Communications* Nov. 2011; **6**(8):628–632.
13. Liao SH, Chen HP, Chiu CC, Liu CL. Channel capacities of indoor MIMO-UWB transmission for different material partitions. *Tamkang Journal of Science and Engineering* Mar. 2011; **14**(1):49–63.
14. Liao SH, Ho MH, Chiu CC. Bit error rate reduction for multiusers by smart UWB Antenna Array. *Progress In Electromagnetic Research C* Sep. 2010; **16**(PIER C 16):85–98.
15. Ho MH, Liao SH, Chiu CC. A novel smart UWB antenna array design by PSO. *Progress In Electromagnetic Research C* Aug. 2010; **15**(PIER C 15):103–115.
16. Ho MH, Liao SH, Chiu CC. UWB communication characteristics for different distribution of people and various materials of walls. *Tamkang Journal of Science and Engineering* Sep. 2010; **13**(3):315–326.
17. Liu CL, Chiu CC, Liao SH, Chen YS. Impact of metallic furniture on UWB channel statistical characteristics. *Tamkang Journal of Science and Engineering* Sep. 2009; **12**(3):271–278.
18. Chen SH, Jeng SK. An SBR/image approach for indoor radio propagation in a corridor. *IEICE Transactions on Electronics* 1995; **E78-C2**:1058–1066.
19. Chen SH, Jeng SK. SBR image approach for radio wave propagation in tunnels with and without traffic. *IEEE Transactions on Vehicular Technology* 1996; **45**:570–578.
20. Loredó S, Rodríguez-Alonso A, Torres RP. Indoor MIMO channel modeling by rigorous GO/UTD-based ray tracing. *IEEE Transactions on Vehicular Technology* Mar. 2008; **57**(2):680–692.
21. Oppermann I, Hamalainen M, Iinatti J. *UWB Theory and Applications*. John Wiley & Sons: UK, 2004.
22. Goldberg DE. Genetic Algorithm in Search. *Optimization and Machine Learning*. Addison Wesley: Reading, Massachusetts, 1989.
23. Michael Johnson J, Rahmat-Samii Y. Genetic algorithms in engineering electromagnetics. *IEEE Antennas and Propagation Magazine* Aug. 1997; **39**(4):7–21.
24. Storn R, Price K. Differential evolution—a simple and efficient adaptive scheme for global optimization over continuous spaces. *Technical Report TR-95-012, International Computer Science Institute, Berkeley*, 1995.
25. Donelli M, Massa A. Computational approach based on a particle swarm optimizer for microwave imaging of two-dimensional dielectric scatterers. *IEEE Transactions on Microwave Theory and Techniques*, May 2005; **53**(5):1761–1776.
26. Zhao Y, Hao Y, Akram A, Clive P. UWB on-body radio channel modeling using ray theory and subband FDTD method. *IEEE Transactions on Microwave Theory and Techniques* 2006; **54**:1827–1835.
27. Buehrer RM, Safaai-Jazi A, Davis W, Sweeney D. Ultra-wideband propagation measurements and modeling. Final Report *DARPA NETEX Program Virginia Tech*, Chapter 3, 2004, 38–216.
28. Muqaibel A, Safaai-Jazi A, Bayram A, Attiya AM, Riad SM. Ultra-wideband through-the-wall propagation. *IEE Proceedings Microwaves, Antennas and Propagation*, 2005, 581–588.
29. Jazi AS, Riad SM, Muqaibel A, Bayram A. Through-the-wall propagation and material characterization. *DARPA NETEX Program Report*, Nov. 2002.
30. Gabriella M, Benedetto D, Giancola G. *Understanding Ultra Wide Band Radio Fundamentals*. Prentice Hall: New Jersey, 2004).
31. Rappaport TS. *Wireless Communications: Principles and Practice*. (2nd edn). Prentice Hall PTR: Upper Saddle River, NJ, USA, 2002).

#### AUTHORS' BIOGRAPHIES



**Shu-Han Liao** was born in Taipei, Taiwan, Republic of China, on September 18, 1982. He received the MSCE degree from Feng Chia University in 2008, and is now working toward his PhD degree in the Department of Electrical Engineering, Tamkang University. His current research interests include indoor wireless communication systems, ultra-wideband systems, and MIMO systems.



**Chien-Ching Chiu** received his BSCE degree from National Chiao Tung University, Hsinchu, Taiwan, in 1985, and his MSEE and PhD degrees from National Taiwan University, Taipei, in 1987 and 1991, respectively. From 1987 to 1989, he was a communication officer with the ROC Army Force. In 1992, he joined the faculty of the Department of Electrical Engineering, Tamkang University, where he is now a professor. From 1998 to 1999, he was a visiting scholar at the Massachusetts Institute of Technology, Cambridge, and the University of Illinois at Urbana-Champaign. He is a visiting professor with the University of Wollongong, Australia, in 2006. Moreover, he was a visiting professor with the University of London, United Kingdom, in 2011.

His current research interests include microwave imaging, numerical techniques in electromagnetics, indoor wireless communications, and ultra-wideband communication systems. He has published more than 109 journal papers on inverse scattering problems, communication systems, and optimization algorithms.



**Min-Hui Ho** was born in Taipei, Taiwan, Republic of China, on March 30, 1983. She received the MSEE and PhD degrees in electrical engineering from Tamkang University, Taipei, Taiwan, in 2007 and 2013, respectively. Her current research interests include indoor wireless communication systems, smart antenna, MIMO systems, optimization methods, and ultra-wideband systems.